

Bio-inspired Distributed Neural Locomotion Controller (D-NLC) for Robust Locomotion and Emergent Behaviors

Zhikai Zhang¹, Siqi Guo², Henry Kou³, Ishayu Shikhare², Howie Choset³, Lu Li³

Abstract—With relatively fewer neurons than more complex life forms, insects are still capable of producing astonishing locomotive behaviors, such as traversing diverse habitats and making rapid gait adaptations after extreme injury or autotomy. Biologists attribute this to a chain of segmental neuron clusters (ganglia) within insect nervous systems, which act as distributed, self-organizing sensorimotor control units. Inspired by the neural structure of the *Carausius morosus*, the common stick insect, this research introduces the Distributed Neural Locomotion Controller (D-NLC), a modular control framework utilizing local proprioceptive feedback to modulate joint-level Central Pattern Generator (CPG) signals to produce emergent locomotive behaviors. We implemented this framework using a modular legged robot with distributed joint-level embedded computing units and assessed its performance and behavior under various experimental settings. Based on real-world experiments, we observe an overall 31.3% average increase in curvilinear motion performance under external (terrain) and internal (amputation) perturbation compared to a centralized predefined gait controller. This difference is statistically significant ($P < 0.05$) for larger perturbations but not for single-leg amputations. Experiments with perturbation-induced leg stance duration and leg-phase-difference analysis further validated our hypothesis regarding D-NLC's role in the robust perceptive locomotion and self-emergent gait adaptation against complex unforeseen perturbations. This proposed control framework does not require any numerical optimization or weight training processes, which are time-consuming and computationally expensive. To the best of our knowledge, this framework is the first bio-inspired neural controller deployed on a distributed embedded system.

I. INTRODUCTION

Animals efficiently perform incredible motions that robots struggle with, such as adapting to unseen terrain and amputation without training or complex computations. Distributed neuron pools throughout the animal body facilitate these behaviors by acting as non-centralized computational units [2], comparable to a network of small microcontrollers (MCU). These neuron pools generate subsequent actions in real time based on local proprioceptive and exteroceptive feedback. This phenomenon can even allow animals to regain their regular functional performance despite severe impairment, such as regaining locomotion by adopting gait changes after leg autotomy, which is widely observed in reptiles and insects [3]. These characteristics are especially beneficial in robotics, enabling task-specific reconfiguration, computational cost reduction, and damage recovery in the field.

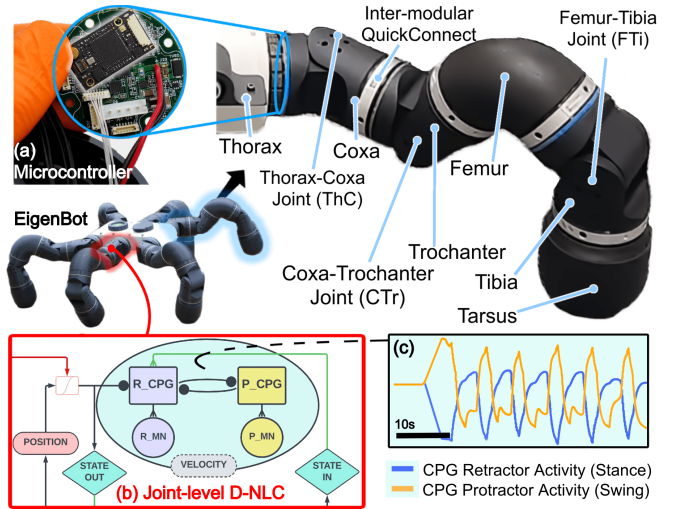


Fig. 1. The bio-inspired Distributed Neural Locomotion Controller (D-NLC) tested on the EigenBot, a novel modular robot prototype, composed of re-configurable joints, each with its own microcontrollers (MCU) (a) to enable distributed computing and tightly-coupled sensorimotor feedback control at the joint-level (b), such as Central Pattern Generator (CPG) retractor/protractor modulating and gait-regulating signal pathways. The EigenBot, in its hexapod configuration, is analogous to the legs and joints of an insect [1]. The joint-level CPG activity (c) during forward walking is illustrated, where the retractor facilitates the stance phase while the protractor modulates swing behavior at the ThC joint. The resulting animal-like behaviors show rapid adaptation against terrain changes and leg amputations without any need for re-programming or training processes. More info at <https://eigenbot-dnlc.github.io>.

Centralized policy that seeks to control the entire body, i.e., all of its degrees-of-freedom (Dof), at once suffers from a deep computational expense, hindering their ability to handle disturbances in real-time that has to rely on time-consuming training (e.g., Reinforcement Learning) [4] or optimization processes [5] (e.g., Optimal Control). Taking inspiration from the invertebrate nervous system, specifically *Carausius morosus* (common stick insect), we introduce Distributed Neural Locomotion Controller (D-NLC) for distributed embedded systems: an unconventional CPG-based control framework physically decentralized into each individual joint module. It can be implemented on a distributed modular robot, shown in Figure 3(a). Unlike existing centralized controllers, which send joint commands to each actuator in a top-down approach, D-NLC is implemented differently: Distributed control on module-level MCUs located in each robotic joint facilitated by inter-module embedded communication. This study shows that with the proposed D-NLC framework, the robot can rapidly adapt to both external (unforeseen terrain) and internal disturbances (various amputations) using the same parameters due to self-emerging animal-like behaviors

¹Department of Mechanical Engineering, Carnegie Mellon University

²Department of Electrical and Computer Engineering, Carnegie Mellon

³Robotics Institute, Carnegie Mellon University (Pittsburgh, PA, USA)

✉ Student Team Lead: zhikaiz@andrew.cmu.edu

✉ PIs: choset@cs.cmu.edu, lilu12@cs.cmu.edu

on a distributed hardware platform.

A. Related Works

Previous works on biologically inspired CPG-based control focus extensively on two main models: spiking neurons and behavior-inspired approaches. Mantisbot [6] and Drosophilobot [7] used spiking neurons to model single-leg functions in simulation and hardware. Nevertheless, these works lack multi-legged full-body implementation or physical robot hardware testing. The Hector robot [8], with muscle-inspired actuators and a Walknet [9] controller, achieved locomotion through reflexes without CPG but was unable to handle complex terrain and leg amputation on hardware. A recurrent neural network and dual-rate learner in [10] could adapt to amputation by predicting foot contact, but this behavior has only been demonstrated in simulation. Its successor paper [11] was able to demonstrate such controller on hardware, but its capability in handling terrain and amputation is not mentioned. A Tegotae-Based controller in [12] demonstrated interlimb coordination on hardware and some amputation adaptation capability, albeit only one configuration, but its terrain handling is not shown. Velocity-based gait changes were implemented with a pacemaker network in [13] using a simplified robot with 2-DoF legs, but amputation or terrain adaptation remains untested. Optimization-based [5] and reinforcement learning methods [4] have performed impressive gait adaptation, but are restricted by predefined models or require time-consuming training processes. Finally, all the above methods rely on a centralized computing system to emulate distributed control, which does not guarantee the feasibility of deployment on a decentralized computing and communication architecture.

In this research, motivated and inspired by several prior works from pioneers, we propose a new approach for a truly distributed sensorimotor control framework: Distributed Neural Locomotion Controller (D-NLC), where both the controller and hardware are distributed to a joint level with no predefined gait or inter-CPG coupling. This paper will summarize our theory, implementation, findings, and lessons learned throughout this research and development exercise.

II. BACKGROUND

A. Insect Leg Mechanics

The insect leg anatomy consists of Thorax-Coxa (ThC), Coxa-Trochanter (CTr), and Femur-Tibia (FTi) joints (see in Figure 1). Position and load-sensitive receptors include femoral chordotonal organs (fCO) and femoral campaniform sensilla (fCS), which influence FTi joint activity, and trochanteral campaniform sensillae (trCS) affecting ThC joint activity. These signals modulate the timing and magnitude of motor outputs [14] [15] [16]. Finally, compliant tarsi significantly facilitate leg contact and force sensing [17].

B. Intralimb Coordination

Networks of CPGs are commonly used to model coordinated rhythmic activity. Findings with insect neuron activation have confirmed the presence of individual loosely

coupled joint CPGs (within ThC, CTr, and FTi joints) in slow-moving insects utilizing mechanosensory feedback, such as the case of the stick insect [18][19][20].

C. Interlimb Coordination

Legs are loosely coupled to each other through a set of interactions known as Cruse's interlimb coordination rules, which have been verified by other works to recreate hexapod insect gaits [21][23]. Interlimb coordination strongly relies on sensory signals, which are mainly active locally between adjacent leg pairs either in the ipsilateral or contralateral direction and affect the coordination of the insect temporally and spatially. Notably, only three of the interlimb rules are vital for primitive hexapod locomotion [9]. Strengths and efficacies of interlimb coupling have been quantified on stick insects' tendencies to enforce a specific rule [24].

D. EigenBot: Prototype for Distributed Locomotion Control

Modular robots can turn a “bag of modules” into a wide variety of special-purpose robots [25]. Modular robots are also the ideal testbed for developing distributed control architecture. The EigenBot robot prototype, developed by the Biorobotics Lab at Carnegie Mellon University (CMU), consists of re-configurable modules equipped with embedded systems that allow distributed computation on ARM Cortex-M-based MCUs (32-bit PSoC™ 5 LP, Infineon Technologies AG) and inter-module communication via Full Duplex RS-485 buses, enabling information sharing to neighboring modules to form tree networks or star networks that follow the physical topology of the robot. EigenBot consists of Several types of modules, such as 1-DoF Rotary Joint Modules made with a modified Dynamixel smart servo (XH430-V350-R, ROBOTIS Co., Ltd.), which can measure joint velocity, position, and torque (via motor current sensing) to provide sensory input for tightly coupled joint level feedback control.

The EigenBot is an 18-DoF hexapod system with three joints per leg to best approximate the six-legged anatomy of *Carausius morosus* (common stick insect) [1]. Motor current signals from EigenBot joints replicates the load conditions of fCS and trCS. Finally, force-sensing foot modules outputs the tarsus's contact state and load estimation. [26].

III. METHOD AND APPROACH

D-NLC coordination can be divided into two categories: intralimb and interlimb pathways, both modulated by joint-level proprioceptive feedback and independent CPGs computed inside each joint's embedded system.

A. Intralimb Coordination Among Joints

Our controller utilizes a Matsuoka oscillator [27], which emulates mutually inhibitory neurons in a non-spiking manner in each joint, shown as yellow units in Figure 2 (d). The CPG units determine the timing of swing and stance muscle activation, while motor neurons (MNs) determine muscle magnitude. Our MN implementation combines muscle and biological MN functionalities into low-level PI joint velocity control on the joint motor, based on leg states: swing, swing-to-stance, stance, and stance-to-swing. Our method extends [14] to a practical hexapod controller.

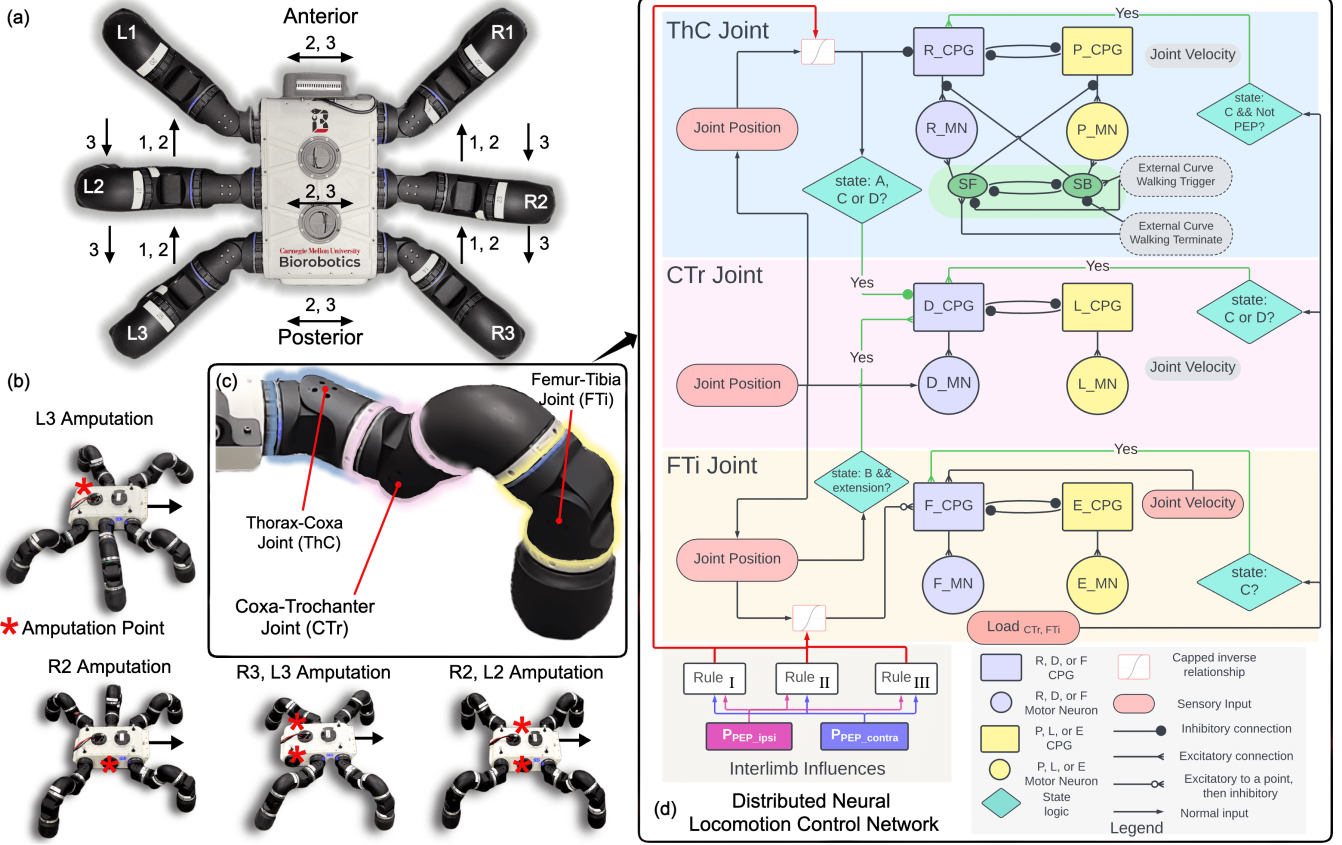


Fig. 2. (a) Rule I,II,III of Cruse’s six interlimb rules and directions of influence are portrayed on the Top-Down view of EigenBot, as referred to in equation 1 [21]. Each leg is labeled with ipsilateral side and contralateral numbering by convention. L1 and R1 represent the most anterior contralateral pair. R2 and R3 represent the right posterior ipsilateral pair. (b) The four amputation configurations were tested with hardware experiments. The robot heading is depicted with the arrow along with locations of the amputation, denoted with (*), at the ThC joints. (c) The EigenBot analogy to an insect leg. Each module is highlighted to correspond to the respective joint-level neural subnetwork implemented in a distributed fashion [1]. (d) leg-level neural control network featuring subnetworks of joint-level CPG nodes interconnected with excitatory and inhibitory edges. ThC joint subnetwork features retractor, protractor CPGs, and motor neurons (MNs) modulated by joint position, leg stance state, and interlimb influences. CTr joint subnetwork features depressor, levator CPGs, and MNs modulated by joint position and leg state. FTi joint subnetwork features flexor, extensor CPGs, and MNs modulated by joint velocity and position, leg state, and interlimb influences. The ThC joint subnetwork also contains additional neurons that facilitate curved walking by interconnecting retractor and protractor MNs. The EigenBot can measure tarsus force with magnetic-based force sensors. [22]. These measurements are currently only used for experimental validation. The first three interlimb influences are based on a percentage of posterior extreme position (PEP) for contralateral and ipsilateral leg pairs. These influences are implemented on the joint level to facilitate a truly distributed control system.

1) Swing Phase Joint Control

This phase succeeds the swing-to-stance phase, where the leg is entirely in the air. This phase ends when the FTi joint extends to its Anterior Extreme Position (AEP) and transitions to swing-to-stance. ThC and FTi joints’ Swing CPGs receive excitatory feedback and are limited by positional limit influences near their Posterior Extreme Position (PEP). The CTr joint’s swing CPG is reduced by the ThC joint’s positional limit influences and vice versa for its stance CPG. CPG output is used to control joint velocity directly.

2) Swing-to-Stance Phase Joint Control

The CTr joint starts depressing at a constant velocity when its stance CPG exceeds its swing CPG. The FTi and ThC joint’s velocity depends on their CPG output. This phase ends with a touch-down sensed by load information on the CTr joint and a transition to the stance phase.

3) Stance Phase and Stance to Swing Phase Joint Control

FTi and ThC joint’s stance CPG is driven down to start flexion and retraction, respectively. The joint motors use velocity control to maintain these motions at a constant ve-

locity. This mirrors stick insect’s behavior in [28], where the assistance reflex quickly raises joint velocity to a threshold and then maintains it. The CTr joint employs height control that adjusts based on the positions of the CTr and FTi joints, ensuring a constant distance between the robot’s body and the ground, represented by “D.MN” in Figure 2. Positional limit influences diminish CTr and ThC joint’s stance CPG as ThC PEP is approached. At the same time, it gives ThC’s swing CPG excitatory influence, causing ThC to cease retraction and CTr to begin levation. The phase transitions to swing when CTr starts levation and loses contact (detected by CTr load feedback). Similarly, the FTi joint stops flexion, but is influenced by its own positional limits. In all three joints, the load signals increase stance CPG, prolonging it, and this can only be reversed by positional limits.

4) Modification to Middle and Hind Leg Controller

The key difference between the mechanism of the middle and hind legs compared to that of the front leg is the FTi joint’s motion. While the front leg’s FTi motion has only flexion during the stance phase, the hind leg only has

extension, and with the middle leg, a combination of both. To achieve the hind leg reverse motion behavior, the PEP and AEP of the hind leg's FTi joint are swapped with respect to the front leg. The middle leg's FTi joint will have flexion in the beginning and extension when the ThC joint has reached its neutral position, halfway between AEP and PEP, as shown in the leg L2 ThC position in Figure 2(a).

B. Interlimb Coordination Rules and Implementation

The Cruse's interlimb coordination rules [21] mainly prolong or shorten the stance&swing phase of each leg. To achieve this, we reduce or increase each leg's PEP or amplitude. Only use *Rule I,II,III*, as they are sufficient to produce stable locomotion [9]. We predefine the amplitude of movement for the ThC and FTi joints along with their AEP and PEP values. Cruse's *Rule I* increases joint amplitude, *Rule II* decreases it, and *Rule III* decreases PEP. Since PEP is limited by amplitude, changing the amplitude proportionally affects PEP. The following formulae represent the rules:

$$\begin{aligned} \text{Rule I: } & A_i = A_i + (1 - P_{pep_i}) \cdot A_i \cdot W_{RuleI} \\ \text{Rule II: } & A_i = A_i - \min(W_{RuleII}, 2) \cdot A_i \\ \text{Rule III: } & PEP_i = A_i - \min(P_{pep_j}, 2) \cdot A_i \cdot W_{RuleIII} \end{aligned} \quad (1)$$

Where i represents the current leg while j represents the influencing leg. A_i is the current leg's amplitude, W_{Rule*} are the weights assigned to each rule, P_{pep_i} is the percentage completion of the current leg's stance stride, P_{pep_j} is the percentage completion of the influencing leg's stance stride. PEP_i is the PEP value of leg i .

The influence of these rules applies to amputation in our implementation, where the previous next neighbor can become the neighboring leg when its immediate neighbor is amputated. (e.g., L1 and L3 become ipsilateral neighbours when L2 is amputated). This differs from the method in [29] where only *Rule I* is propagated.

IV. EXPERIMENT AND RESULTS

The performance of D-NLC is evaluated through adaptation to perturbation and is compared to a predefined tripod gait using a centralized controller. It is tested in simulation on flat and uneven terrain and transferred to hardware. In hardware experiments, the robot walks forward for 60s under D-NLC or a predefined tripod gait ($N=5$). Motion capture data of the robot's center body is recorded at 100 Hz using an OptiTrack system, along with stance-swing phase data for each leg. Tests include flat ground, terrain, and various amputations (L3, R2, R2+L2, R3+L3) as shown in 2 (b).

A. D-NLC Outperforms Predefined Tripod Gait in Handling Perturbations

The controller's performance is assessed by the decrease in tangential velocity. The overall torso velocity's projection onto the robot's x-axis at each timestamp is calculated from motion capture data (position and orientation) shown in Figure 3 (a) to evaluate its ability to walk straight under different perturbations, thus demonstrating adaptability. Figure 3 (f) shows the percentage decrease of flat walking

velocity. D-NLC has significantly less velocity decrease than predefined tripod gait under every perturbation ($P=0.00296 \sim 0.00350$) except for L3 amputation ($P=0.111$) and R2 amputation ($P=0.274$). This result indicates that the D-NLC adapts dramatically better than predefined gait for larger perturbations, such as two-leg amputation. The result is less convincing for smaller perturbations, such as one-leg amputation. The predefined gait has a significant velocity decrease due to its inability to modify gait, causing excessive turning or a general inability to move.

B. D-NLC Produces Emergent Behavior under Perturbations

The emergent behaviors of a hexapod can be represented by interactions between legs (interlimb coordination) and within each leg (intralimb coordination). Interlimb coordination is shown by phase differences. Raw stance/swing phase data (Figure 3 (d)) appears as a square wave and is pre-processed with a low-pass filter due to low gait cycle frequency. Cross-spectrum density (CSD) analysis identifies the highest correlated frequencies between two phase data sets. We select the frequency with the largest peak magnitude-squared coherence within 0.09-0.23 Hz, consistent with observed gait frequencies. Figure 3 (e) shows phase differences at these frequencies between two legs. Absolute phase (θ) values closer to π indicate more anti-phase behavior, while values near 0 indicate more in-phase behavior. During flat walking, neighboring legs (e.g., R1-R2, R1-L1) show more anti-phase behavior ($\pi/2 < \theta < \pi$), while non-neighboring legs are more in-phase ($0 < \theta < \pi/2$), resembling a tripod gait. After R2 amputation, R1 and R3, previously in-phase, become out-of-phase. Figure 3(e) provides an alternative view, logging swing probability for each leg, with similar-shaped legs grouped into alternating sinusoidal patterns.

Swing probability is calculated using R1 as a reference:

$$P([\phi = 1]|t - t_{1 \rightarrow 0}) = \frac{1}{N} \sum_{n=1}^N \sum_{i=1}^W \frac{[\phi = 1]|t^{ni} - t_{1 \rightarrow 0}^{ni}|}{W} \quad (2)$$

Where ϕ represents the phase (1 for swing, 0 for stance), $t_{1 \rightarrow 0}$ is the time of the touch-down event of R1, W is the number of R1's swing-to-stance transitions in a trial, and N is the number of trials.

In contrast with predefined gait, D-NLC's emergent behavior enabled straighter walking and reduced excessive turning. In R2+L2 and R3+L3 amputations, diagonal legs moved closer in phase, forming a trotting-like gait. In terrain experiments, phase differences had a larger SD (e.g., 0.378π in R3-L3), with R1-R3 more anti-phase due to increased load on R3 while climbing. This behavior extended R3's stance phase, providing better support and preventing slippage.

The stance duration increased on rough terrain and post-amputation, as shown in Figure 4 (e) for R1. Amputations caused longer stance phases ($P = 0.00397 \sim 0.0278$) due to shifted weight distribution. Terrain experiments showed less statistical significance ($P=0.0754$) as R1 experienced less load on slopes, where the hind legs bore more weight due to a positive torso pitch angle.

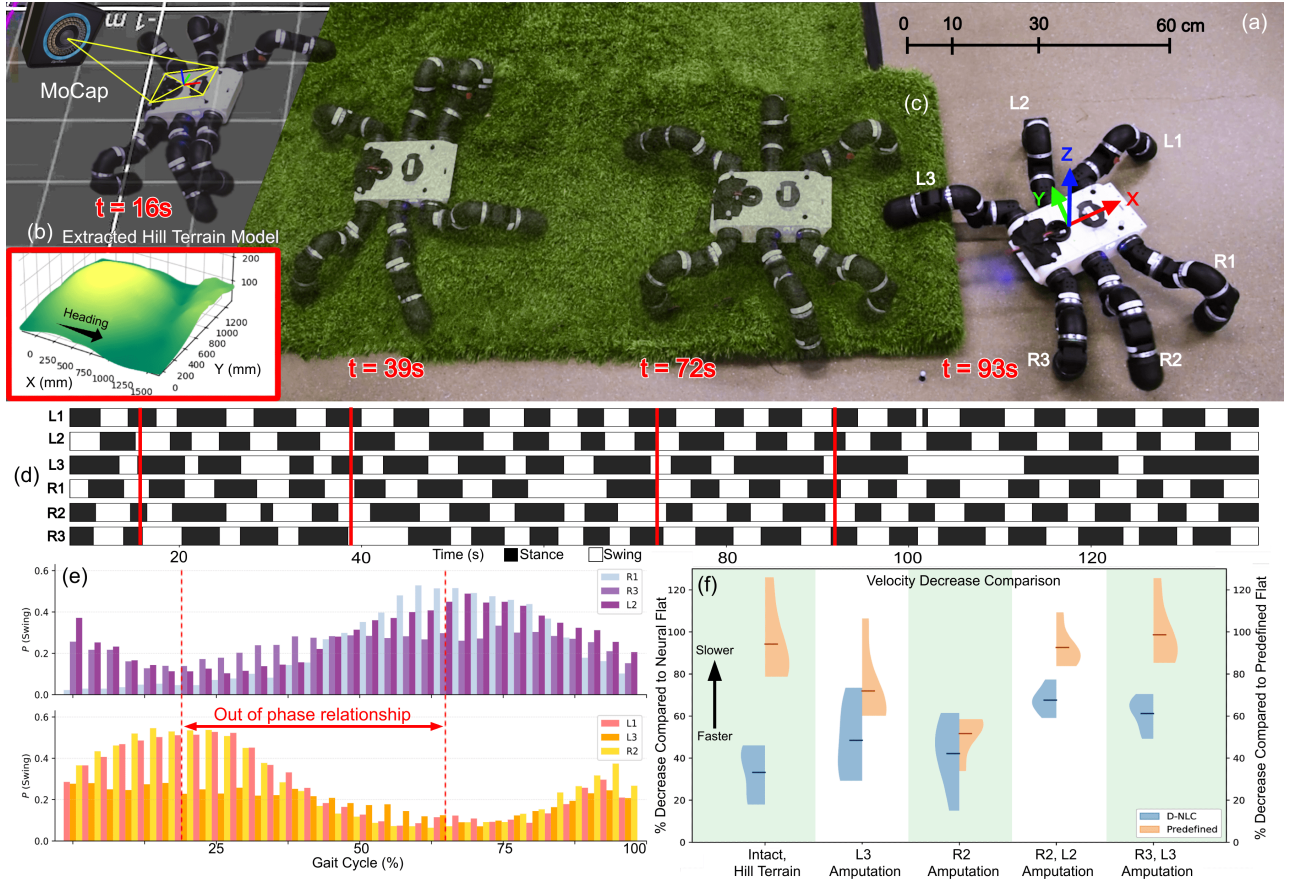


Fig. 3. Experimental setup with motion capture and gait & Forward Velocity analysis (a) Motion capture OptiTrack system is used to record center body pose for gait and stability analysis at 100Hz, where the robot traverses constructed physical terrain (height map visualized in (b)). (b) Terrain dimensions are approximately 1.5x1.2 m and 10 cm peak height. The hill structure contains two peaks (c) Full six-leg D-NLC traverses the terrain and internal end effector stance and swing phase signals are recorded as a gait plot (d). Time stamps at 16s, 39s, 72s, and 93s show the internal state of end effector phases, respectively. (e) Analysis on gait phases shows a convergence of tripod gait over time with distributions of swing probability (Equation 2) clustering high for R1, R3, and L2 leg groups and low swing probability for L1, L3, and R2 leg groups. (f) Comparisons between D-NLC and a centralized predefined gait controller show that D-NLC experiences less percentage decrease (Ave. 31.3%) in forward tangential velocity with respect to intact flat walking for every perturbation experiment. This indicates the robustness of D-NLC locomotion under the terrain and amputation perturbation. The violin plot illustrates the distribution of velocity decrease, with wider sections indicating a higher density of data points and horizontal lines marking the mean.

V. DISCUSSION

A. D-NLC Performance Assessment

D-NLC adapts better to internal (amputations) and external (hill terrain) perturbations than to a predefined gait while maintaining gait pattern and speed. The percentage of velocity decrease, shown in Figure 3, indicates that the behavior of D-NLC is relatively unaffected by perturbation in the cases of flat walking, terrain and amputation.

B. Observation on Emergent behaviors

Adaptive behaviors emerge through proprioceptive feedback and interlimb influences during locomotive performance. Especially demonstrated with amputation, the shifted swing-stance phase patterns of D-NLC reflect the internal redirection of interlimb influences among remaining legs to improve stability and maintain locomotion. Note, this behavior is absent in predefined gait, leading to excessive turning or an inability to move forward. Increasing phase difference between previous in-phase leg pairs is also observed in biological amputation studies in various hexapod

insects, where the average front and hind leg phase difference changed from 0.5π to π with R2+L2 amputation [30][3].

C. Comparison to Biology and The EigenBot Platform

Insights into insect neural structures can be gained through a comparison of robot and biological data. Rule I is modified in [29], where with L2 amputation, L3 directs its Rule I influence towards L1. We added Rule II and Rule III between L1 and L3, producing anti-phase behavior between the legs on a distributed hardware platform. This result suggests possible bidirectional communication between nonadjacent legs and a mechanism redirecting proprioceptive influences based on leg configuration. Further experiments on insects are needed to confirm these hypothetical mechanisms.

The EigenBot facilitates this comparison by implementing an intuitive platform for bio-inspired control. D-NLC is distributed across each hardware module, mimicking distributed neural architectures in biology, thus providing more accurate constraints and structure, such as communication delays similar to insect biology[31].

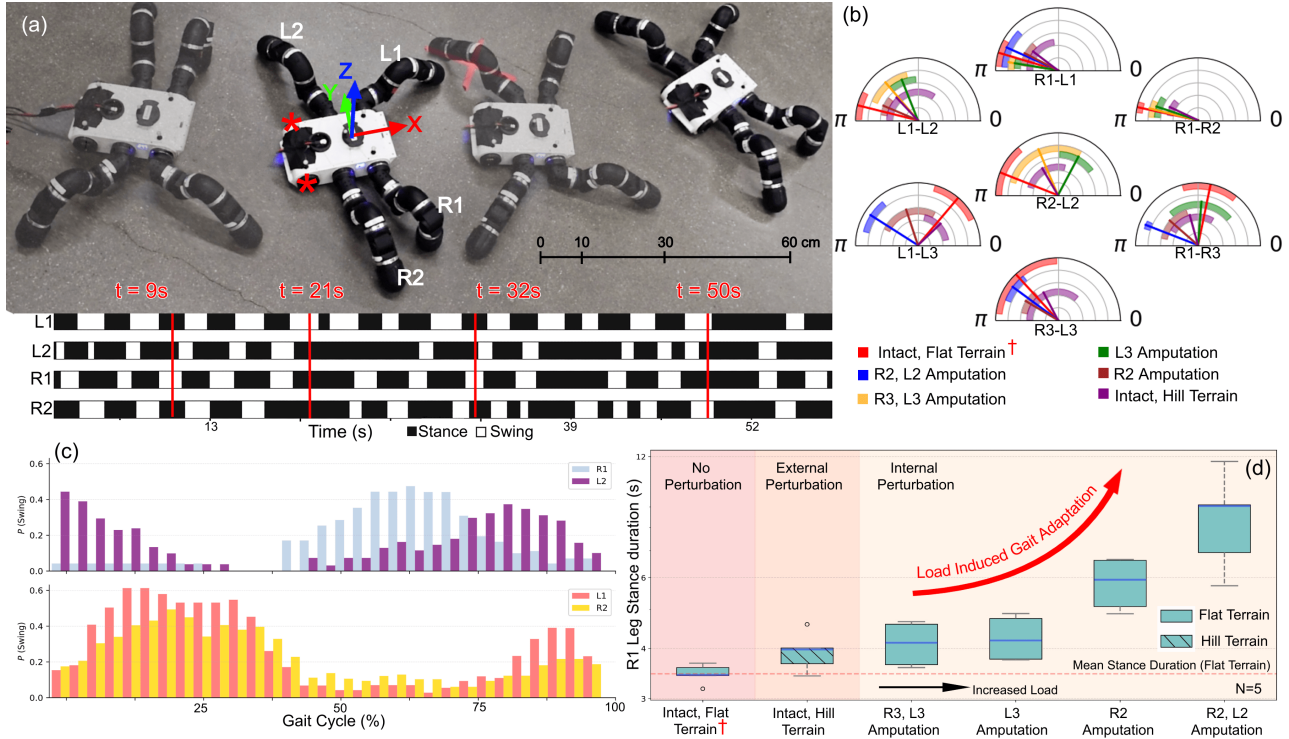


Fig. 4. Amputation experimental setup and emergent behavior analysis (a) EigenBot running on D-NLC with R3-L3 amputation. Time stamps at 9s, 21s, 32s, and 50s show the internal state of end effector phases, respectively. Internal end effector stance and swing phase signals for four legs on flat is recorded in the gait plot. (b) Shows the phase difference diagrams. Shown in the half-polar plots are the mean and standard deviation of absolute phase difference in each leg pair's relationships. The phase difference between legs changes with changing amputation configurations and terrain. Phase differences vs. the baseline of intact, flat terrain walking (\dagger) shows that amputations do lead to changes in leg coordination. (c) Swing Probability by 2 illustrates the phase difference among the four legs. When the robot has been amputated, the adjacent legs maintain the out-of-phase relationship as an emergent gait to produce forward locomotion. This relationship is shown in the alternating peaks of R1 and L2 vs. L1 and R2 over the robot's gait cycle. (d) Stance duration of leg R1 of different experiments, ordered in increasing load experienced, with a baseline of intact flat terrain walking(\dagger). Hill terrain is shown to have a longer stance duration with less statistical significance ($P=0.075$). Amputation of the legs also shows a longer stance phase adaptation ($P=0.00397 \sim 0.0278$).

D. Limitations and Future Work

While producing emergent behaviors, D-NLC cannot perfectly mimic insect locomotion behavior (e.g., stability) due to 1) unknown feedback functions, 2) rigid height control, 3) lack of complete locomotion behaviors, 4) turning issues from imperfect leg coordination, and (5) complex parameter tuning. Sensory influence can be represented by a weight, but designing its feedback function is challenging. Additionally, the height controller uses simple negative feedback with a constant height reference. In insect locomotion, height is a function of tarsus force [32]. Despite demonstrating only forward walking, curve walking and turn-in-place for D-NLC have been tested in simulation by adding a neuron and the corresponding interconnections (see in SB and SF neurons in Figure 2(d)) to the existing modular framework. This highlights the potential for extendability in D-NLC, which will be further evaluated on hardware. Lastly, the parameter space is large, making tuning cumbersome based on live observation of the robot behavior. Future work includes modeling the proprioceptive feedback function with biological data to obtain insights into insect control mechanisms, which can allow for physical intuition and simplifications behind the parameter space. In addition, adding tactile tarsus sensors inspired by [26],[33] for adaptive height control and optimal foot placement, adding better sim-to-real pipeline, and open-sourcing this research for community collaboration.

VI. CONCLUSION

In the bio-inspired robotic design community, there is an inherent consideration and debate between the level of detail in biological inspiration and functionality, often due to technological limitations. Currently, a large portion of biological details (e.g., stick insect neural dynamics at a cellular level) are unknown, leading to the failure of a functional system of bio-inspired locomotion when only the high-level structural part is modeled. This work presents a promising, simplistic, and practical embedded control framework achieving adaptive control against internal and external perturbations through emergent behaviors on a truly distributed robot system. Results show the controller's robustness against perturbation and emergent gait adaptation capability under amputations. Comparing these results with biology validates the controller's implementation.

ACKNOWLEDGMENTS

We would like to thank all CMU Biorobotics Lab members, especially the EigenBot engineering team (Nick Paiva, Mike Schwerin, G Jaya Aadityaa, Joshua Spisak, Junpei Ma), and experiment team (Greg Armstrong, Ye Jin, Cindy Fu). Authors' contributions: ZZ: D-NLC lead, firmware (FW), experiments (EXP), paper/figure (P/F); SG: FW, EXP, P/F; HK: EXP, P/F; IS: P/F; LL: Robot design, P/F; HC: P/F.

REFERENCES

- [1] A. Biewener and S. Patek, “Animal locomotion: Oxford university press,” 2003.
- [2] T. Buschmann, A. Ewald, A. von Twickel, and A. Büschges, “Controlling legs for locomotion—insights from robotics and neurobiology,” *Bioinspir. Biomim.*, vol. 10, no. 4, p. 041001, June 2015.
- [3] F. Delcomyn, “The effect of limb amputation on locomotion in the cockroach *Periplaneta Americana*,” *J. Exp. Biol.*, vol. 54, no. 2, pp. 453–469, Apr. 1971.
- [4] X. Cheng, K. Shi, A. Agarwal, and D. Pathak, “Extreme parkour with legged robots,” *CoRL*, Sept. 2023.
- [5] J. Whitman, S. Su, S. Coros, A. Ansari, and H. Choset, “Generating gaits for simultaneous locomotion and manipulation,” in *2017 IEEE/RSJ International Conference on Intelligent Robots and Systems (IROS)*. IEEE, Sept. 2017. [Online]. Available: <http://dx.doi.org/10.1109/IROS.2017.8206099>
- [6] N. S. Szczecinski, D. M. Chrzanowski, D. W. Cofer, D. R. Moore, A. S. Terrasi, J. P. Martin, R. E. Ritzmann, and R. D. Quinn, “Mantisbot: A platform for investigating mantis behavior via real-time neural control,” in *Biomimetic and Biohybrid Systems: 4th International Conference, Living Machines 2015, Barcelona, Spain, July 28–31, 2015, Proceedings 4*. Springer, 2015, pp. 175–186.
- [7] C. Goldsmith, N. Szczecinski, and R. Quinn, “Drosophilobot: a fruit fly inspired bio-robot,” in *Biomimetic and Biohybrid Systems: 8th International Conference, Living Machines 2019, Nara, Japan, July 9–12, 2019, Proceedings 8*. Springer, 2019, pp. 146–157.
- [8] A. Schneider, J. Paskarbeit, M. Schaeffermann, and J. Schmitz, “Hector, a new hexapod robot platform with increased mobility-control approach, design and communication,” in *Advances in Autonomous Mini Robots: Proceedings of the 6-th AMIRE Symposium*. Springer, 2012, pp. 249–264.
- [9] H. Cruse, T. Kindermann, M. Schumm, J. Dean, and J. Schmitz, “Walknet—a biologically inspired network to control six-legged walking,” *Neural Networks*, vol. 11, no. 7–8, pp. 1435–1447, 1998. [Online]. Available: [https://doi.org/10.1016/s0893-6080\(98\)00067-7](https://doi.org/10.1016/s0893-6080(98)00067-7)
- [10] A. Miguel-Blanco and P. Manoonpong, “General distributed neural control and sensory adaptation for self-organized locomotion and fast adaptation to damage of walking robots,” *Front. Neural Circuits*, vol. 14, p. 46, Aug. 2020.
- [11] T. Sun, Z. Dai, and P. Manoonpong, “Robust and reusable self-organized locomotion of legged robots under adaptive physical and neural communications,” *Front. Neural Circuits*, vol. 17, p. 1111285, Mar. 2023.
- [12] D. Owaki, M. Goda, S. Miyazawa, and A. Ishiguro, “A minimal model describing hexapedal interlimb coordination: The tegotae-based approach,” *Front. Neurorobot.*, vol. 11, p. 29, June 2017.
- [13] H. Chiel, R. Beer, R. Quinn, and K. Espenschied, “Robustness of a distributed neural network controller for locomotion in a hexapod robot,” *IEEE Transactions on Robotics and Automation*, vol. 8, no. 3, p. 293–303, June 1992. [Online]. Available: <http://dx.doi.org/10.1109/70.143348>
- [14] Ö. Ekeberg, M. Blümel, and A. Büschges, “Dynamic simulation of insect walking,” *Arthropod structure & development*, vol. 33, no. 3, pp. 287–300, 2004.
- [15] A. Buschges, “Sensory control and organization of neural networks mediating coordination of multisegmental organs for locomotion,” *Journal of neurophysiology*, vol. 93, no. 3, pp. 1127–1135, 2005.
- [16] T. Akay, U. Bassler, P. Gerharz, and A. Buschges, “The role of sensory signals from the insect coxa-trochanteral joint in controlling motor activity of the femur-tibia joint,” *Journal of neurophysiology*, vol. 85, no. 2, pp. 594–604, 2001.
- [17] T. Akay, S. Haehn, J. Schmitz, and A. Buschges, “Signals from load sensors underlie interjoint coordination during stepping movements of the stick insect leg,” *Journal of neurophysiology*, vol. 92, no. 1, pp. 42–51, 2004.
- [18] A. Büschges and M. Gruhn, “Mechanosensory feedback in walking: from joint control to locomotor patterns,” *Advances in insect physiology*, vol. 34, pp. 193–230, 2007.
- [19] S. Daun-Gruhn and A. Büschges, “From neuron to behavior: dynamic equation-based prediction of biological processes in motor control,” *Biological cybernetics*, vol. 105, pp. 71–88, 2011.
- [20] S. S. Bidaye, T. Bockemühl, and A. Büschges, “Six-legged walking in insects: how cpgs, peripheral feedback, and descending signals generate coordinated and adaptive motor rhythms,” *Journal of neurophysiology*, vol. 119, no. 2, pp. 459–475, 2018.
- [21] V. Dürr, J. Schmitz, and H. Cruse, “Behaviour-based modelling of hexapod locomotion: linking biology and technical application,” *Arthropod structure & development*, vol. 33, no. 3, pp. 237–250, 2004.
- [22] K. Dai, X. Wang, A. M. Rojas, E. Harber, Y. Tian, N. Paiva, J. Gnehm, E. Schindewolf, H. Choset, V. A. Webster-Wood, and L. Li, “Design of a biomimetic tactile sensor for material classification,” in *Proceedings of (ICRA) International Conference on Robotics and Automation*, May 2022.
- [23] M. Schilling, T. Hoiville, J. Schmitz, and H. Cruse, “Walknet, a bio-inspired controller for hexapod walking,” *Biological cybernetics*, vol. 107, pp. 397–419, 2013.
- [24] V. Durr, “Context-dependent changes in strength and efficacy of leg coordination mechanisms,” *Journal of experimental biology*, vol. 208, no. 12, pp. 2253–2267, 2005.
- [25] J. S. Whitman, “Automating automation with modular robot synthesis,” Ph.D. dissertation, Carnegie Mellon University, 2022.
- [26] E. Harber, E. Schindewolf, V. Webster-Wood, H. Choset, and L. Li, “A tunable magnet-based tactile sensor framework,” in *2020 IEEE SENSORS*, 2020, pp. 1–4.
- [27] G. Liu *et al.*, “Central pattern generators based on matsuoka oscillators for the locomotion of biped robots,” *Artificial Life and Robotics*, vol. 12, no. 1–2, pp. 264–269, 2008.
- [28] U. Bässler and A. Büschges, “Pattern generation for stick insect walking movements—multisensory control of a locomotor program,” *Brain Research Reviews*, vol. 27, no. 1, pp. 65–88, 1998. [Online]. Available: [https://doi.org/10.1016/s0165-0173\(98\)00006-x](https://doi.org/10.1016/s0165-0173(98)00006-x)
- [29] M. Schilling, H. Cruse, and P. Arena, “Hexapod walking: an expansion to walknet dealing with leg amputations and force oscillations,” *Biological Cybernetics*, vol. 96, no. 3, p. 323–340, Nov. 2006. [Online]. Available: <http://dx.doi.org/10.1007/s00422-006-0117-1>
- [30] D. Owaki, H. Aonuma, Y. Sugimoto, and A. Ishiguro, “Leg amputation modifies coordinated activation of the middle leg muscles in the cricket *gryllus bimaculatus*,” *Sci. Rep.*, vol. 11, no. 1, p. 1327, Jan. 2021.
- [31] C. Gebehart and A. Büschges, “Temporal differences between load and movement signal integration in the sensorimotor network of an insect leg,” *J. Neurophysiol.*, vol. 126, no. 6, pp. 1875–1890, Dec. 2021.
- [32] H. Cruse, J. Schmitz, U. Braun, and A. Schweins, “Control of body height in a stick insect walking on a treadmill,” *J. Exp. Biol.*, vol. 181, no. 1, pp. 141–155, Aug. 1993.
- [33] K. Dai, X. Wang, A. M. Rojas, E. Harber, Y. Tian, N. Paiva, J. Gnehm, E. Schindewolf, H. Choset, V. A. Webster-Wood, and L. Li, “Design of a biomimetic tactile sensor for material classification,” in *2022 International Conference on Robotics and Automation (ICRA)*. IEEE, May 2022.